Vaccine hesitancy promotes emergence of new SARS-CoV-2 variants

Shuanglin Jing [a,1], Russell Milne [b,1], Hao Wang [b,*], Ling Xue [a]

[a] *College of Mathematical Sciences, Harbin Engineering University, Harbin, Heilongjiang, 150001, China*
[b] *Department of Mathematical and Statistical Sciences & Interdisciplinary Lab for Mathematical Ecology and Epidemiology, University of Alberta, Edmonton, Alberta T6G 2R3, Canada*

ARTICLE INFO

ABSTRACT

The successive emergence of SARS-CoV-2 mutations has led to an unprecedented increase in COVID-19 incidence worldwide. Currently, vaccination is considered to be the best available solution to control the ongoing COVID-19 pandemic. However, public opposition to vaccination persists in many countries, which can lead to increased COVID-19 caseloads and hence greater opportunities for vaccine-evasive mutant strains to arise. To determine the extent that public opinion regarding vaccination can induce or hamper the emergence of new variants, we develop a model that couples a compartmental disease transmission framework featuring two strains of SARS-CoV-2 with game theoretical dynamics on whether or not to vaccinate. We combine semi-stochastic and deterministic simulations to explore the effect of mutation probability, perceived cost of receiving vaccines, and perceived risks of infection on the emergence and spread of mutant SARS-CoV-2 strains. We find that decreasing the perceived costs of being vaccinated and increasing the perceived risks of infection (that is, decreasing vaccine hesitation) will decrease the possibility of vaccine-resistant mutant strains becoming established by about fourfold for intermediate mutation rates. Conversely, we find increasing vaccine hesitation to cause both higher probability of mutant strains emerging and more wild-type cases after the mutant strain has appeared. We also find that once a new variant has emerged, perceived risk of being infected by the original variant plays a much larger role than perceptions of the new variant in determining future outbreak characteristics. Furthermore, we find that rapid vaccination under non-pharmaceutical interventions is a highly effective strategy for preventing new variant emergence, due to interaction effects between non-pharmaceutical interventions and public support for vaccination. Our findings indicate that policies that combine combating vaccine-related misinformation with non-pharmaceutical interventions (such as reducing social contact) will be the most effective for avoiding the establishment of harmful new variants.

1. Introduction

The ongoing COVID-19 pandemic presents great threats to public health and significant challenges to global economic development. Since the identification of the first case of SARS-CoV-2 in December 2019, the COVID-19 pandemic has caused more than 649 million confirmed cases worldwide and a number of confirmed deaths above 6.6 million as of December 19, 2022 (World Health Organization, 2022). The rapid mutation rate of the COVID-19 virus is one of the main driving factors for its huge and long-lasting impact, as it has led to the development of many different SARS-CoV-2 variants, which have caused multiple COVID-19 outbreak waves worldwide (Xue et al., 2022). These include the Delta variant (B.1.617.2), which was discovered in Maharashtra, India in October 2020 and subsequently caused a major outbreak both in that country and globally (Del Rio et al.,

2021), and the Omicron variant (B.1.1.529), which was first discovered in Gauteng, South Africa in November 2021 and went on to produce even greater global case numbers than Delta (Maslo et al., 2022; Planas et al., 2022). Since its initial emergence, the Omicron variant has continued mutating, giving rise to multiple sublineages (e.g., BA.1.1, BA.2, BA.2.12.1, BA.5, BQ.1, and BQ.1.1) (Elliott et al., 2022; Centers for Disease Control and Prevention, 2022; Tegally et al., 2022) that have caused prolonged periods of high COVID-19 transmission rates in many countries. The CDC expects that new variants of SARS-CoV-2 will continue to emerge (Centers for Disease Control and Prevention, 2022), in part because of the virus's high mutation ability.

The SARS-CoV-2 variants that have emerged recently have higher transmission rates than both the 2009 H1N1 strain of influenza and its seasonal varieties (Xue et al., 2022; Faust and Del Rio, 2020). This increase in transmissibility has led to the need for a stronger response

---

by governments and individuals to reduce SARS-CoV-2 infection. As the global outbreak of COVID-19 has progressed, it has become clear that many non-pharmaceutical interventions (such as lockdowns) are not economically and socially sustainable in the long run (Lobinska et al., 2022). Therefore, vaccination is considered to be the best available solution to control the ongoing COVID-19 pandemic (Rella et al., 2021), as it facilitates mortality reduction by way of providing large portions of the population with immunity. Hence, vaccinated populations can avoid large-scale infections and potentially achieve herd immunity, meaning that vaccination can at least theoretically eradicate COVID-19 (Lobinska et al., 2022; Rella et al., 2021). However, this possibility of eradication has faced challenges from the successive emergence of SARS-CoV-2 variants (Tegally et al., 2021). Many studies have shown that in addition to their higher infectivity, the new SARS-CoV-2 variants have stronger immune evasion (Thompson et al., 2021), making them resistant to the original vaccines developed for wild-type SARS-CoV-2 (McCallum et al., 2021; Cai et al., 2021; Cao et al., 2022). Additionally, as vaccination rates increase, those who have not been vaccinated become steadily less likely to be infected due to herd immunity (Brisson and Edmunds, 2003). This makes more and more individuals refuse to be vaccinated, since non-vaccinators can be protected through herd immunity without the risk of vaccine complications (Bauch, 2005).

Mathematical models can be used to understand the successive emergence of SARS-CoV-2 variants and help inform effective vaccination strategies. Many modelling studies have hence been performed to make projections about the emergence and spread of these variants (Lobinska et al., 2022; Rella et al., 2021; Bordon, 2022; Gandon and Lion, 2022; McLeod and Gandon, 2022). For instance, Rella et al. used a stochastic SIR-derived model of SARS-CoV-2 transmission to investigate the impact of vaccination rates and the intensity of non-pharmaceutical interventions on the probability of a vaccine-resistant strain emerging, and hence to simulate the different outbreak waves inherent in the pandemic (Rella et al., 2021). Lobinska et al. used a transmission model to analyze the evolutionary dynamics of SARS-CoV-2 mutations, in the context of both changes in contact patterns over the course of the pandemic and the speed of vaccine rollout (Lobinska et al., 2022). Their results show that if vaccination happens slowly, vaccine-resistant mutant strains of SARS-CoV-2 are likely to emerge even if social distancing is adhered to. Conversely, when vaccines are delivered to a population quickly, the emergence of vaccine-resistant strains can be prevented if the public continues to adhere to social distancing practices during the vaccination campaign (Lobinska et al., 2022).

However, as the SARS-CoV-2 pandemic wears on, persistent vaccine hesitancy may emerge in populations in the same way it has with other diseases (e.g. measles Lo and Hotez, 2017). This would render it much more challenging to prevent the emergence of harmful new mutant strains that could repeat the serious damage seen earlier in the pandemic. Over the course of a disease's time infecting human populations, the perceived risks of vaccines and infection by the disease change due to the interplay between vaccine coverage, disease prevalence, and opinions on vaccines among the population at large (Bauch, 2005). Concerns on vaccine safety, underestimation of infection risk, and anticipation of herd immunity can all lead to a dramatic drop in vaccination rates (Poland and Jacobson, 2001). These critical factors governing long-term vaccination dynamics (and hence variant emergence) have rarely been considered in the previous literature on SARS-CoV-2 mutations. Nevertheless, doing so is crucial now that the development and rollout of COVID-19 vaccines is done on a more regular schedule and countries make longer-term COVID-19 management plans. Because of this, we developed a model of disease transmission featuring two strains (a wild-type and a vaccine-resistant mutant) that joins compartmental transmission dynamics with game theory. Within this model, individuals make decisions on vaccination according to disease prevalence (i.e. the number of new cases) and the perceived risks of vaccines and disease, allowing us to address questions of how these decisions can affect the shape of a COVID-19 outbreak.

In our simulations, we use both semi-stochastic and deterministic simulations to uncover how social behaviour related to vaccination affects the dynamics of our model. We simulate the effects of mutation probability and the perceived risks from being infected or receiving vaccine doses on the probability of producing a vaccine-resistant mutant strain of SARS-CoV-2. To assess the impact of these perceived costs on the burden of COVID-19 (measured in terms of the daily number of new cases), we run simulations for different values of the perceived cost of vaccination, as well as the perceived risks of infection by a contemporaneously dominant, or wild-type, strain of SARS-CoV-2 and a vaccine-resistant mutant strain. This includes simulations in which non-pharmaceutical interventions are applied, in order to determine the strength of the interaction effect on pandemic mitigation between these interventions and a population supportive of vaccination.

2. Materials and methods

In this section, we introduce an infectious disease model with two mutant strains and vaccination, taking the form of a homogeneous system of ordinary differential equations. For simplification, we assume that there are no births, as well as no deaths unrelated to COVID-19.

2.1. Disease prevalence model

To mimic the spread of the COVID-19 epidemic, we incorporate vaccination into a disease transmission model. We divide the whole population into twelve classes: susceptible individuals $S(t)$; vaccinated individuals $V(t)$; individuals exposed to SARS-CoV-2, divided into those exposed to wild-type SARS-CoV-2 (hereafter denoted "WT") $E_{WT}(t)$ and those exposed to a vaccine-resistant mutant type of SARS-CoV-2 (hereafter denoted "MT") $E_{MT}(t)$; pre-symptomatic infectious individuals, divided into those infected with WT $P_{WT}(t)$ and those infected with MT $P_{MT}(t)$; asymptomatic infectious individuals, divided into those infected with WT $A_{WT}(t)$ and those infected with MT $A_{MT}(t)$; symptomatic infectious individuals, divided into those infected with WT $I_{WT}(t)$ and those infected with MT $I_{MT}(t)$; recovered individuals $R(t)$; and individuals who die of the infection $D(t)$. The total population is denoted by N, where $N = S + V + E_{WT} + E_{MT} + P_{WT} + P_{MT} + A_{WT} + A_{MT} + I_{WT} + I_{MT} + R$. The forces of infection for WT and MT (among susceptible and vaccinated individuals) are defined as

$$\lambda_i = \beta_i(\theta_i P_i + \delta_i A_i + I_i), \quad i = \{WT, MT\},$$

where δ_i and θ_i, $i = \{WT, MT\}$ govern the probabilities of transmission in asymptomatic and pre-symptomatic individuals, respectively, relative to symptomatic individuals. β_{WT} and β_{MT} denote the transmission rate of WT and MT. Our disease transmission model is therefore formulated as follows:

$$\frac{dS}{dt} = -\frac{\lambda_{WT} S}{N} - \frac{\lambda_{MT} S}{N} - pxS + \tau V,$$

$$\frac{dV}{dt} = pxS - \frac{\lambda_{WT} \eta_{WT} V}{N} - \frac{\lambda_{MT} \eta_{MT} V}{N} - \tau V,$$

$$\frac{dE_{WT}}{dt} = \frac{\lambda_{WT} \left[(1 - u_S)S + (1 - u_V)\eta_{WT} V \right]}{N} - \sigma_{WT} E_{WT},$$

$$\frac{dE_{MT}}{dt} = \frac{\lambda_{WT}(u_S S + u_V \eta_{WT} V)}{N} + \frac{\lambda_{MT}(S + \eta_{MT} V)}{N} - \sigma_{MT} E_{MT},$$

$$\frac{dP_{WT}}{dt} = \sigma_{WT} E_{WT} - \alpha_{WT} P_{WT},$$

$$\frac{dP_{MT}}{dt} = \sigma_{MT} E_{MT} - \alpha_{MT} P_{MT}, \tag{1}$$

$$\frac{dA_{WT}}{dt} = \rho_{WT} \alpha_{WT} P_{WT} - \gamma_{A_{WT}} A_{WT},$$

$$\frac{dA_{MT}}{dt} = \rho_{MT} \alpha_{MT} P_{MT} - \gamma_{A_{MT}} A_{MT},$$

$$\frac{dI_{WT}}{dt} = (1 - \rho_{WT})\alpha_{WT}P_{WT} - \gamma_{I_{WT}}I_{WT},$$

$$\frac{dI_{MT}}{dt} = (1 - \rho_{MT})\alpha_{MT}P_{MT} - \gamma_{I_{MT}}I_{MT},$$

$$\frac{dR}{dt} = \mu_{WT}\gamma_{I_{WT}}I_{WT} + \mu_{MT}\gamma_{I_{MT}}I_{MT} + \gamma_{A_{WT}}A_{WT} + \gamma_{A_{MT}}A_{MT},$$

$$\frac{dD}{dt} = (1 - \mu_{WT})\gamma_{I_{WT}}I_{WT} + (1 - \mu_{MT})\gamma_{I_{MT}}I_{MT}.$$

In the above model, p represents the vaccination rate, while x represents the proportion of the population willing to receive a vaccine. (Not all individuals in the population will be vaccinated after $1/p$ days, necessitating the inclusion of x). $1/\tau$ represents the maximum duration of vaccine protection. u_S and u_V are the probability that WT will undergo a mutation in unvaccinated and vaccinated individuals, respectively. Additionally, both WT and MT are associated with several quantities related to their infectivity and mortality. These are probability of death among symptomatic individuals $1 - \mu_i$, mean incubation period length $1/\sigma_i$, mean infectious period lengths $1/\alpha_i$ for pre-symptomatic individuals, mean infectious period lengths $1/\gamma_{A_i}$ for asymptomatic individuals and $1/\gamma_{I_i}$ for symptomatic individuals, and proportion of infected individuals that are asymptomatic ρ_i, where the values for WT are denoted by $i = WT$ and those for MT are denoted by $i = MT$. Similarly, η_{MT} and η_{WT} denote the reduction in susceptibility conferred by vaccination to WT and MT, respectively (i.e. how effective a vaccine series is against contracting COVID-19); these take values between 0 and 1. If $\eta_{MT} = 1$, then vaccination confers no immunity to MT, meaning that MT escapes completely. For $0 < \eta_{MT} < 1$, MT is a partial escape mutant. For $\eta_{MT} = 0$, MT does not escape at all.

2.2. Game theoretical vaccination model

During an epidemic, individuals are exposed to many often conflicting pieces of information about how severe the circulating disease is, how likely they are to get it, and the efficacy of available vaccines. Because of this, the perceived risks of the disease in question and being vaccinated for it vary over time. Hence, the proportion of individuals willing to be vaccinated (we will call these "vaccinators"), represented above as x, is dynamic. Therefore, we use imitation dynamics drawn from evolutionary game theory to simulate human decisions whether or not to vaccinate, as well as the downstream impact of these decisions on the emergence of mutant strains (Bauch and Earn, 2004; Bauch, 2005; Pananos et al., 2017; Deka and Bhattacharyya, 2022). This is accomplished by defining functions for the perceived utility that an individual receives when following a strategy of vaccination or non-vaccination; here, these take the form of utility costs related to getting vaccinated or being vulnerable to COVID-19. Let F_v be the utility function for vaccinators. Since our model formulation focuses on utility costs, this function is related to the risk of adverse effects from the vaccine. Hence, we define F_v as

$$F_v = -r_v,$$

where r_v is the perceived cost of being vaccinated or the perceived probability of morbidity caused by the vaccine.

Likewise, in our model formulation, the utility function for non-vaccinators F_n contains the cost associated with not being vaccinated. Intuitively, this represents the perceived cost associated with SARS-CoV-2 infection, meaning that it depends on the number of infected individuals. Within our model, SARS-CoV-2 infections can be due to either WT or MT, and can further be either symptomatic or asymptomatic, meaning that F_n will depend on I_{WT}, I_{MT}, A_{WT} and A_{MT}. Assuming that the perceived cost of not being vaccinated scales linearly with case numbers, we can describe the cost of (for instance) symptomatic infection by WT using the term $r_{I_{WT}}I_{WT}$, where the constant $r_{I_{WT}}$ is the perceived personal danger from such an infection. Furthermore, since people decide to be vaccinators or non-vaccinators depending on the relative magnitudes of F_v and F_n (in other words, the

risk due to getting the vaccine versus the risk due to being infected by SARS-CoV-2), we introduce an additional constant $m_{I_{WT}}$ in this term to describe how sensitive individual behaviour regarding vaccination is to fluctuations in case count. This makes the term for the perceived cost of symptomatic infection by WT equal to $r_{I_{WT}}m_{I_{WT}}I_{WT}$. Similar analysis gives us terms of $r_{I_{MT}}m_{I_{MT}}I_{MT}$, $r_{A_{WT}}m_{A_{WT}}A_{WT}$, and $r_{A_{MT}}m_{A_{MT}}A_{MT}$ for symptomatic infection by MT and asymptomatic infection by WT and MT, respectively. Hence, the perceived utility for a strategy of non-vaccination can be expressed as

$$F_n(A_{WT}, A_{MT}, I_{WT}, I_{MT}) = -\left(r_{A_{WT}}m_{A_{WT}}A_{WT} + r_{A_{MT}}m_{A_{MT}}A_{MT} \right.$$
$$\left. + r_{I_{WT}}m_{I_{WT}}I_{WT} + r_{I_{MT}}m_{I_{MT}}I_{MT} \right).$$

Individuals decide whether to vaccinate through a social learning or imitation process. Suppose individuals hear the opinions regarding vaccination of other members of the population, randomly sampled, at some constant rate. The more positive the payoff for some individual's strategy, the higher the probability that another member of the population that interacts with that individual will adopt their strategy. In other words, individuals following a lower payoff strategy that hear about a higher payoff strategy may shift to it (Bauch, 2005; Pharaon and Bauch, 2018; Deka and Bhattacharyya, 2022). Thus, the payoff gain for switching to a vaccination strategy is

$$\Delta F = F_v - F_n(A_{WT}, A_{MT}, I_{WT}, I_{MT}).$$

Note that individuals tend to switch their strategy, provided other members of the population who have adopted a different strategy receive a higher payoff (Deka et al., 2020). If the payoff for vaccinators is greater than that for non-vaccinators ($\Delta F > 0$), then non-vaccinators may become vaccinators. (Since F_v and F_n are both negative or zero, $\Delta F > 0$ means that F_n is more negative than F_v, indicating a higher cost for the non-vaccination strategy.) Conversely, if $\Delta F < 0$, people who had previously committed to being vaccinated would instead choose not to be, and thus frequency of vaccinators would decrease. We let x denote the proportion of vaccinators, meaning that $(1 - x)$ denotes the proportion of non-vaccinators, and that positive change in x indicates more people becoming vaccinators. If individuals sample the population at a rate ϕ, then any individual doing this would sample vaccinators at rate ϕx. If a non-vaccinator does so and is exposed to the opinions of vaccinators, they will switch to the vaccinator strategy with probability $\omega \Delta F$, where ω is a proportionality constant that includes the chance of switching after hearing different opinions (Bauch, 2005). The case describing vaccinators switching to being non-vaccinators is symmetrical, as the proportion of the total population consisting of vaccinators is x and they will sample non-vaccinators at a rate $\phi(1 - x)$. Accordingly, the evolutionary equation describing the proportion of vaccinators can be defined as follows:

$$\frac{dx}{dt} = (1 - x)\phi x \omega \Delta F, \qquad (2)$$

For simplicity, we let $k = \phi\omega$, where k is the combined imitation rate at which individuals sample others and switch strategies. Then, Eq. (2) is simplified into

$$\frac{dx}{dt} = kx(1 - x)\Delta F. \qquad (3)$$

Hence, our model is rewritten as follows:

$$\frac{dS}{dt} = -\frac{\lambda_{WT}S}{N} - \frac{\lambda_{MT}S}{N} - pxS + \tau V,$$

$$\frac{dV}{dt} = pxS - \frac{\lambda_{WT}\eta_{WT}V}{N} - \frac{\lambda_{MT}\eta_{MT}V}{N} - \tau V,$$

$$\frac{dE_{WT}}{dt} = \frac{\lambda_{WT}\left[(1 - u_S)S + (1 - u_V)\eta_{WT}V\right]}{N} - \sigma_{WT}E_{WT},$$

$$\frac{dE_{MT}}{dt} = \frac{\lambda_{WT}(u_S S + u_V \eta_{WT}V)}{N} + \frac{\lambda_{MT}(S + \eta_{MT}V)}{N} - \sigma_{MT}E_{MT},$$

$$\frac{dP_{WT}}{dt} = \sigma_{WT}E_{WT} - \alpha_{WT}P_{WT},$$

$$\frac{dP_{MT}}{dt} = \sigma_{MT}E_{MT} - \alpha_{MT}P_{MT},$$

$$\frac{dA_{WT}}{dt} = \rho_{WT}\alpha_{WT}P_{WT} - \gamma_{A_{WT}}A_{WT}, \tag{4}$$

$$\frac{dA_{MT}}{dt} = \rho_{MT}\alpha_{MT}P_{MT} - \gamma_{A_{MT}}A_{MT},$$

$$\frac{dI_{WT}}{dt} = (1-\rho_{WT})\alpha_{WT}P_{WT} - \gamma_{I_{WT}}I_{WT},$$

$$\frac{dI_{MT}}{dt} = (1-\rho_{MT})\alpha_{MT}P_{MT} - \gamma_{I_{MT}}I_{MT},$$

$$\frac{dR}{dt} = \mu_{WT}\gamma_{I_{WT}}I_{WT} + \mu_{MT}\gamma_{I_{MT}}I_{MT} + \gamma_{A_{WT}}A_{WT} + \gamma_{A_{MT}}A_{MT},$$

$$\frac{dD}{dt} = (1-\mu_{WT})\gamma_{I_{WT}}I_{WT} + (1-\mu_{MT})\gamma_{I_{MT}}I_{MT},$$

$$\frac{dx}{dt} = kx(1-x)\Delta F.$$

It should be noted that the vaccination dynamics in Model (4) imply that the waiting time to vaccination is exponentially distributed. This represents vaccines being readily available and hence most people being able to receive one quickly, as has been the case in the latter stages of the COVID-19 pandemic. If vaccines instead became scarce and required rationing, alternative approaches that involve placing maximum numerical values on the flow from S to V per unit time could be used.

According to Model (4), the daily numbers of new cases for WT and MT are formulated as

$$C^{WT}(i) = \int_{\text{day } i} \alpha_{WT}P_{WT}(t)dt$$

and

$$C^{MT}(i) = \int_{\text{day } i} \alpha_{MT}P_{MT}(t)dt,$$

respectively. Thus, the overall daily number of new cases is $C(i) = C^{WT}(i) + C^{MT}(i)$.

Cases in unvaccinated and vaccinated individuals can be estimated as

$$U_c(t) = \frac{\lambda_{WT}(t)S(t)}{N(t)} + \frac{\lambda_{MT}(t)S(t)}{N(t)}$$

and

$$V_c(t) = \frac{\lambda_{WT}(t)\eta_{WT}V(t)}{N(t)} + \frac{\lambda_{MT}(t)\eta_{MT}V(t)}{N(t)},$$

respectively. Although this uses the number of people entering the exposed states rather than the number of people entering the symptomatic and asymptomatic infectious states, it produces the same proportions of unvaccinated and vaccinated cases as if the latter number was used. This is because exposed and pre-symptomatic individuals cannot die of COVID-19 or receive vaccines in our model, so the proportions of unvaccinated and vaccinated individuals in the early stages of SARS-CoV-2 infection remain constant as said individuals advance through these stages.

The effective reproduction number in this model is defined as the maximum of that of WT and that of MT (see Appendix A), specifically as

$$R_e(t) = \max\left\{ R_e^{WT}(t), R_e^{MT}(t) \right\}, \tag{5}$$

where

$$R_e^{WT}(t) = \frac{(1-u_S)S(t) + (1-u_V)\eta_{WT}V(t)}{N(t)}$$
$$\times \left(\frac{\beta_{WT}\theta_{WT}}{\alpha_{WT}} + \frac{\beta_{WT}\rho_{WT}\delta_{WT}}{\gamma_{A_{WT}}} + \frac{\beta_{WT}(1-\rho_{WT})}{\gamma_{I_{WT}}} \right),$$

$$R_e^{MT}(t) = \frac{S(t) + \eta_{MT}V(t)}{N(t)}$$
$$\times \left(\frac{\beta_{MT}\theta_{MT}}{\alpha_{MT}} + \frac{\beta_{MT}\rho_{MT}\delta_{MT}}{\gamma_{A_{MT}}} + \frac{\beta_{MT}(1-\rho_{MT})}{\gamma_{I_{MT}}} \right).$$

Above, $\beta_{WT}\theta_{WT}$ ($\beta_{MT}\theta_{MT}$), $\beta_{WT}\delta_{WT}$ ($\beta_{MT}\delta_{MT}$), and β_{WT} (β_{MT}) represent the probabilities of contact transmission per unit time between pre-symptomatic, asymptomatic, and symptomatic individuals infected by WT (MT) and susceptible individuals, respectively. $1/\alpha_{WT}$ ($1/\alpha_{MT}$), $1/\gamma_{A_{WT}}$ ($1/\gamma_{A_{MT}}$), and $1/\gamma_{I_{WT}}$ ($1/\gamma_{I_{MT}}$) are the average times that pre-symptomatic, asymptomatic, and symptomatic individuals infected by WT (MT) remain infectious. The term $1-\rho_{WT}$ ($1-\rho_{MT}$) is equivalent to $\alpha_{WT}(1-\rho_{WT})/\alpha_{WT}$ ($\alpha_{MT}(1-\rho_{MT})/\alpha_{MT}$), which is the proportion of individuals that have been infected with WT (MT) and are in the pre-symptomatic stage that progress to the symptomatic stage. Similarly, a proportion $\alpha_{WT}\rho_{WT}/\alpha_{WT}$ ($\alpha_{MT}\rho_{MT}/\alpha_{MT}$) of individuals in the pre-symptomatic stage of WT (MT) infection instead progress to the asymptomatic stage. Additionally, for each individual that can spread the virus (pre-symptomatic, symptomatic and asymptomatic), $S(t)/N(t)$ represents the probability of effective contact with susceptible individuals at time t. Similarly, $\eta_{WT}V(t)/N(t)$ and $\eta_{MT}V(t)/N(t)$ represent the probability of effective contact with vaccinated individuals at time t for individuals infected by WT and MT, respectively, since the probability of transmission to vaccinated individuals is scaled down by the constants η_{WT} and η_{MT}. We also have, in effect, $R_e^{WT}(t) \leq R_0^{WT}$ and $R_e^{MT}(t) \leq R_0^{MT}$, since we took nearly the entire population to be susceptible at the beginning of our simulations. Since $S(t)$, $V(t)$, and $N(t)$ are time-varying during the course of an epidemic, $R_e^{WT}(t)$ and $R_e^{MT}(t)$ are also considered to be time-varying metrics (Zhao et al., 2022).

2.3. Semi-stochastic simulation

As the emergence of new variants of COVID-19 can be viewed as a stochastic process, we developed a stochastic model (Gillespie, 1977) to simulate this. To accomplish this, we took S, V, E_{WT}, E_{MT}, P_{WT}, P_{MT}, A_{WT}, A_{MT}, I_{WT}, I_{MT}, R, and D to be discrete variables, considered all of the rates in Model (4) that cause individuals in the population to be transferred between the groups designated by these variables, and converted these rates into 32 randomly occurring events. These events hence represent state transitions in Model (4), and are shown in Table 1. Since x is on a different order of magnitude than the other variables, which are expressed as population numbers, we use semi-stochastic simulation for ease of computation. In other words, within our semi-stochastic simulation, x is deterministic and the other variables are treated stochastically (Xiao et al., 2006; Wang et al., 2012). Further detail on our semi-stochastic method, such as how we used the probabilities in Table 1 to generate time series, may be found in Appendix B.

When simulating the emergence of new variants, we performed multiple stochastic simulations and averaged the time series thus generated, from which we obtained average numbers of new daily cases of WT and MT (see Results section).

2.4. Parameter estimation

We fixed some of the parameters in Model (4) based on previous studies (Li et al., 2020a; Qiu, 2020; Li et al., 2020b; Hao et al., 2020; Kumar et al., 2021; Tang et al., 2022). Since the incubation period of COVID-19 is around 5.2 days (Li et al., 2020a), we took the mean length of incubation period of both WT and MT to be 5.2 days, meaning that $1/\sigma_{WT}+1/\alpha_{WT} = 1/\sigma_{MT}+1/\alpha_{MT} = 5.2$. We assumed a pre-symptomatic infectious period of $1/\alpha_{WT} = 1/\alpha_{MT} = 2.3$ days (Hao et al., 2020). Thus the latent period was $1/\sigma_{WT} = 1/\sigma_{MT} = 2.9$ days. Moreover, we assumed that the average recovery periods for symptomatic and asymptomatic infected individuals for the two variants are 11 and 7 days (Kumar et al., 2021; Tang et al., 2022), respectively, leading to $\gamma_{I_{WT}} = \gamma_{I_{MT}} = 1/11$ and $\gamma_{A_{WT}} = \gamma_{A_{MT}} = 1/7$ per day. Around $30\%-90\%$ of people infected with due to COVID-19 are asymptomatic or only have mild symptoms; within this subpopulation, SARS-CoV-2 transmissibility is lower, but still significant (Qiu, 2020; Dong et al., 2020; Mizumoto

Table 1
Events and their rates of the stochastic model.

Event	Change of transition state	Rate	Probability in $[t, t + dt]$
S is infected by P_{WT} (no mutation)	$(S, E_{WT}) \rightarrow$ $(S - 1, E_{WT} + 1)$	$T_1 = \frac{(1-u_S)\beta_{WT}\theta_{WT}P_{WT}S}{N}$	$\frac{(1-u_S)\beta_{WT}\theta_{WT}P_{WT}S dt}{N}$
S is infected by P_{WT} (mutation)	$(S, E_{MT}) \rightarrow$ $(S - 1, E_{MT} + 1)$	$T_2 = \frac{u_S\beta_{WT}\theta_{WT}P_{WT}S}{N}$	$\frac{u_S\beta_{WT}\theta_{WT}P_{WT}S dt}{N}$
S is infected by A_{WT} (no mutation)	$(S, E_{WT}) \rightarrow$ $(S - 1, E_{WT} + 1)$	$T_3 = \frac{(1-u_S)\beta_{WT}\delta_{WT}A_{WT}S}{N}$	$\frac{(1-u_S)\beta_{WT}\delta_{WT}A_{WT}S dt}{N}$
S is infected by A_{WT} (mutation)	$(S, E_{MT}) \rightarrow$ $(S - 1, E_{MT} + 1)$	$T_4 = \frac{u_S\beta_{WT}\delta_{WT}A_{WT}S}{N}$	$\frac{u_S\beta_{WT}\delta_{WT}A_{WT}S dt}{N}$
S is infected by I_{WT} (no mutation)	$(S, E_{WT}) \rightarrow$ $(S - 1, E_{WT} + 1)$	$T_5 = \frac{(1-u_S)\beta_{WT}I_{WT}S}{N}$	$\frac{(1-u_S)\beta_{WT}I_{WT}S dt}{N}$
S is infected by I_{WT} (mutation)	$(S, E_{MT}) \rightarrow$ $(S - 1, E_{MT} + 1)$	$T_6 = \frac{u_S\beta_{WT}I_{WT}S}{N}$	$\frac{u_S\beta_{WT}I_{WT}S dt}{N}$
S is infected by P_{MT}	$(S, E_{MT}) \rightarrow$ $(S - 1, E_{MT} + 1)$	$T_7 = \frac{\beta_{MT}\theta_{MT}P_{MT}S}{N}$	$\frac{\beta_{MT}\theta_{MT}P_{MT}S dt}{N}$
S is infected by A_{MT}	$(S, E_{MT}) \rightarrow$ $(S - 1, E_{MT} + 1)$	$T_8 = \frac{\beta_{MT}\delta_{MT}A_{MT}S}{N}$	$\frac{\beta_{MT}\delta_{MT}A_{MT}S dt}{N}$
S is infected by I_{MT}	$(S, E_{MT}) \rightarrow$ $(S - 1, E_{MT} + 1)$	$T_9 = \frac{\beta_{MT}I_{MT}S}{N}$	$\frac{\beta_{MT}I_{MT}S dt}{N}$
Movement from S to V	$(S, V) \rightarrow$ $(S - 1, V + 1)$	$T_{10} = pxS$	$pxS dt$
Movement from V to S	$(S, V) \rightarrow$ $(S + 1, V - 1)$	$T_{11} = \tau V$	$\tau V dt$
V is infected by P_{WT} (no mutation)	$(V, E_{WT}) \rightarrow$ $(V - 1, E_{WT} + 1)$	$T_{12} = \frac{(1-u_V)\beta_{WT}\theta_{WT}P_{WT}\eta_{WT}V}{N}$	$\frac{(1-u_V)\beta_{WT}\theta_{WT}P_{WT}\eta_{WT}V dt}{N}$
V is infected by P_{WT} (mutation)	$(S, E_{MT}) \rightarrow$ $(V - 1, E_{MT} + 1)$	$T_{13} = \frac{u_V\beta_{WT}\theta_{WT}P_{WT}\eta_{WT}V}{N}$	$\frac{u_V\beta_{WT}\theta_{WT}P_{WT}\eta_{WT}V dt}{N}$
V is infected by A_{WT} (no mutation)	$(V, E_{WT}) \rightarrow$ $(V - 1, E_{WT} + 1)$	$T_{14} = \frac{(1-u_V)\beta_{WT}\delta_{WT}A_{WT}\eta_{WT}V}{N}$	$\frac{(1-u_V)\beta_{WT}\delta_{WT}A_{WT}\eta_{WT}V dt}{N}$
V is infected by A_{WT} (mutation)	$(V, E_{MT}) \rightarrow$ $(V - 1, E_{MT} + 1)$	$T_{15} = \frac{u_V\beta_{WT}\delta_{WT}A_{WT}\eta_{WT}V}{N}$	$\frac{u_V\beta_{WT}\delta_{WT}A_{WT}\eta_{WT}V dt}{N}$
V is infected by I_{WT} (no mutation)	$(V, E_{WT}) \rightarrow$ $(V - 1, E_{WT} + 1)$	$T_{16} = \frac{(1-u_V)\beta_{WT}I_{WT}\eta_{WT}V}{N}$	$\frac{(1-u_V)\beta_{WT}I_{WT}\eta_{WT}V dt}{N}$
V is infected by I_{WT} (mutation)	$(V, E_{MT}) \rightarrow$ $(V - 1, E_{MT} + 1)$	$T_{17} = \frac{u_V\beta_{WT}I_{WT}\eta_{WT}V}{N}$	$\frac{u_V\beta_{WT}I_{WT}\eta_{WT}V dt}{N}$
V is infected by P_{MT}	$(V, E_{MT}) \rightarrow$ $(V - 1, E_{MT} + 1)$	$T_{18} = \frac{\beta_{MT}\theta_{MT}P_{MT}\eta_{MT}V}{N}$	$\frac{\beta_{MT}\theta_{MT}P_{MT}\eta_{MT}V dt}{N}$
V is infected by A_{MT}	$(V, E_{MT}) \rightarrow$ $(V - 1, E_{MT} + 1)$	$T_{19} = \frac{\beta_{MT}\delta_{MT}A_{MT}\eta_{MT}V}{N}$	$\frac{\beta_{MT}\delta_{MT}A_{MT}\eta_{MT}V dt}{N}$
V is infected by I_{MT}	$(V, E_{MT}) \rightarrow$ $(V - 1, E_{MT} + 1)$	$T_{20} = \frac{\beta_{MT}I_{MT}\eta_{MT}V}{N}$	$\frac{\beta_{MT}I_{MT}\eta_{MT}V dt}{N}$
Movement from E_{WT} to P_{WT}	$(E_{WT}, P_{WT}) \rightarrow$ $(E_{WT} - 1, P_{WT} + 1)$	$T_{21} = \sigma_{WT}E_{WT}$	$\sigma_{WT}E_{WT} dt$
Movement from E_{MT} to P_{MT}	$(E_{MT}, P_{MT}) \rightarrow$ $(E_{MT} - 1, P_{MT} + 1)$	$T_{22} = \sigma_{MT}E_{MT}$	$\sigma_{MT}E_{MT} dt$
Movement from P_{WT} to A_{WT}	$(P_{WT}, A_{WT}) \rightarrow$ $(P_{WT} - 1, A_{WT} + 1)$	$T_{23} = \rho_{WT}\alpha_{WT}P_{WT}$	$\rho_{WT}\alpha_{WT}P_{WT} dt$
Movement from P_{WT} to I_{WT}	$(P_{WT}, I_{WT}) \rightarrow$ $(P_{WT} - 1, I_{WT} + 1)$	$T_{24} = (1 - \rho_{WT})\alpha_{WT}P_{WT}$	$(1 - \rho_{WT})\alpha_{WT}P_{WT} dt$
Movement from P_{MT} to A_{MT}	$(P_{MT}, A_{MT}) \rightarrow$ $(P_{MT} - 1, A_{MT} + 1)$	$T_{25} = \rho_{MT}\alpha_{MT}P_{MT}$	$\rho_{MT}\alpha_{MT}P_{MT} dt$
Movement from P_{MT} to I_{MT}	$(P_{MT}, I_{MT}) \rightarrow$ $(P_{MT} - 1, I_{MT} + 1)$	$T_{26} = (1 - \rho_{MT})\alpha_{MT}P_{MT}$	$(1 - \rho_{MT})\alpha_{MT}P_{MT} dt$
Recovery from A_{WT}	$(A_{WT}, R) \rightarrow$ $(A_{WT} - 1, R + 1)$	$T_{27} = \gamma_{A_{WT}}A_{WT}$	$\gamma_{A_{WT}}A_{WT} dt$
Recovery from A_{MT}	$(A_{MT}, R) \rightarrow$ $(A_{MT} - 1, R + 1)$	$T_{28} = \gamma_{A_{MT}}A_{MT}$	$\gamma_{A_{MT}}A_{MT} dt$
Recovery from I_{WT}	$(I_{WT}, R) \rightarrow$ $(I_{WT} - 1, R + 1)$	$T_{29} = \mu_{WT}\gamma_{I_{WT}}I_{WT}$	$\mu_{WT}\gamma_{I_{WT}}I_{WT} dt$
Death from I_{WT}	$(I_{WT}, D) \rightarrow$ $(I_{WT} - 1, D + 1)$	$T_{30} = (1 - \mu_{WT})\gamma_{I_{WT}}I_{WT}$	$(1 - \mu_{WT})\gamma_{I_{WT}}I_{WT} dt$

(continued on next page)

Table 1 (*continued*).

Event	Change of transition state	Rate	Probability in $[t, t+\mathrm{d}t]$
Recovery from I_{MT}	$(I_{MT}, R) \rightarrow$ $(I_{MT} - 1, R + 1)$	$T_{31} = \mu_{MT}\gamma_{I_{MT}}I_{MT}$	$\mu_{MT}\gamma_{I_{MT}}I_{MT}\mathrm{d}t$
Death from I_{MT}	$(I_{MT}, D) \rightarrow$ $(I_{MT} - 1, D + 1)$	$T_{32} = (1 - \mu_{MT})\gamma_{I_{MT}}I_{MT}$	$(1 - \mu_{MT})\gamma_{I_{MT}}I_{MT}\mathrm{d}t$

Table 2
Definitions and values of parameters.

Parameters	Description	Value	Source
$\frac{1}{\sigma_{WT}}$ and $\frac{1}{\sigma_{MT}}$	The mean length of latent period	2.9	Li et al. (2020a) and Hao et al. (2020)
$\frac{1}{\alpha_{WT}}$ and $\frac{1}{\alpha_{MT}}$	The pre-symptomatic infectious period	2.3	Li et al. (2020a) and Hao et al. (2020)
$\frac{1}{\gamma_{I_{WT}}}$ and $\frac{1}{\gamma_{I_{MT}}}$	The symptomatic infectious period	11	Kumar et al. (2021)
$\frac{1}{\gamma_{A_{WT}}}$ and $\frac{1}{\gamma_{A_{MT}}}$	The asymptomatic infectious period	7	Tang et al. (2022)
ρ_{WT} and ρ_{MT}	The proportion of asymptomatic infected individuals	60%	Qiu (2020), Dong et al. (2020), Mizumoto et al. (2020), Akinbami et al. (2022) and Murray (2022)
θ_{WT} and θ_{MT}	The factor for reduced transmission probability of asymptomatic infected individuals	0.55	Li et al. (2020b) and Hao et al. (2020)
δ_{WT} and δ_{MT}	The factor for reduced transmission probability of pre-symptomatic individuals	0.55	Li et al. (2020b) and Hao et al. (2020)
$1/\tau$	The maximum duration of vaccine protection	240	Yang et al. (2021), Al Kaabi et al. (2021), Thomas et al. (2021), Barouch et al. (2021) and Pegu et al. (2021)
β_{WT}	The transmission rate of WT	0.2	Assumed
β_{MT}	The transmission rate of MT	0.4	Assumed
$1 - \mu_{WT}$	Probability of death from infection with WT	0.01	Assumed
$1 - \mu_{MT}$	Probability of death from infection with MT	0.005	Assumed
$1 - \eta_{WT}$	Protection level of vaccine against WT	0.8	Assumed
$1 - \eta_{MT}$	Protection level of vaccine against MT	0.2	Assumed
p	The vaccination rate	0.05	Assumed
k	The combined imitation rate at which individuals sample others and switch strategies	0.2	Assumed
$m_{A_{WT}}$	The sensitivity of vaccinating behaviour to changes in prevalence of asymptomatic individuals infected with WT	0.04	Assumed
$m_{A_{MT}}$	The sensitivity of vaccinating behaviour to changes in prevalence of asymptomatic individuals infected with MT	0.04	Assumed
$m_{I_{WT}}$	The sensitivity of vaccinating behaviour to changes in prevalence of symptomatic individuals infected with WT	0.07	Assumed
$m_{I_{MT}}$	The sensitivity of vaccinating behaviour to changes in prevalence of symptomatic individuals infected with MT	0.07	Assumed

et al., 2020; Akinbami et al., 2022; Murray, 2022). Thus, we assumed that the probabilities of an infected individual being asymptomatic are $\rho_{WT} = \rho_{MT} = 60\%$, and we set $\theta_{WT} = \theta_{MT} = \delta_{WT} = \delta_{MT} = 0.55$ (Li et al., 2020b; Hao et al., 2020) due to lower transmissibility among both exposed and asymptomatic infected individuals. Several studies have shown that the effectiveness of COVID-19 vaccine decreases significantly after 6 to 8 months (Yang et al., 2021; Al Kaabi et al., 2021; Thomas et al., 2021; Barouch et al., 2021; Pegu et al., 2021), therefore, we assumed that the maximum duration of vaccine protection is $1/\tau = 8 \times 30$ days. For the infectivity of the two variants, we assumed that MT is more infective than WT (Xue et al., 2022; Cao et al., 2022; Cele et al., 2022), leading to the assumption that $\beta_{MT} > \beta_{WT}$. According to results on the fatality of SARS-CoV-2 mutations (Xue et al., 2022), we assumed that MT is less fatal than WT, so we took $1 - \mu_{WT} > 1 - \mu_{MT}$. Lower viral loads in the vaccinated individuals could lead to fewer mutations (Grenfell et al., 2004; Gutierrez and Gog, 2023), therefore, we assumed that $u_S > u_V$. In addition, without loss of generality, we also assumed that MT has stronger immune evasion ability (Xue et al., 2022). This implies that the vaccine has a lower protection rate against

MT compared with WT, in other words $\eta_{MT} > \eta_{WT}$. All parameters are listed in Table 2.

3. Results

In this section, we perform semi-stochastic simulations of Model (4) to illustrate the impact of human decision on vaccination on the emergence and spread of MT. These simulations are carried out using parameter values that are drawn either from the literature, estimated from available information or through reasonable guesses. Unless otherwise specified, the parameter values used for simulations are the ones listed in Section 2.4, as well as $\eta_{WT} = 0.2$, $\eta_{MT} = 0.8$, $\beta_{WT} = 0.2$, $\beta_{MT} = 0.4$, $p = 0.05$, $1 - \mu_{WT} = 0.01$, $1 - \mu_{MT} = 0.005$, $k = 0.2$, $m_{A_{WT}} = m_{A_{MT}} = 0.04$, and $m_{I_{WT}} = m_{I_{MT}} = 0.07$. The initial values used for the simulations are $S(0) = 9986$, $V(0) = 0$, $E_{WT}(0) = 5$, $E_{MT}(0) = 0$, $P_{WT}(0) = 5$, $P_{MT}(0) = 0$, $A_{WT}(0) = 2$, $A_{MT}(0) = 0$, $I_{WT}(0) = 2$, $I_{MT}(0) = 0$, $R(0) = 0$, $D(0) = 0$, and $x(0) = 0.1$. In particular, the initial values $E_{MT}(0) = 0$, $P_{MT}(0) = 0$, $A_{MT}(0) = 0$, and $I_{MT}(0) = 0$ indicate that the MT has not been produced at the beginning of the
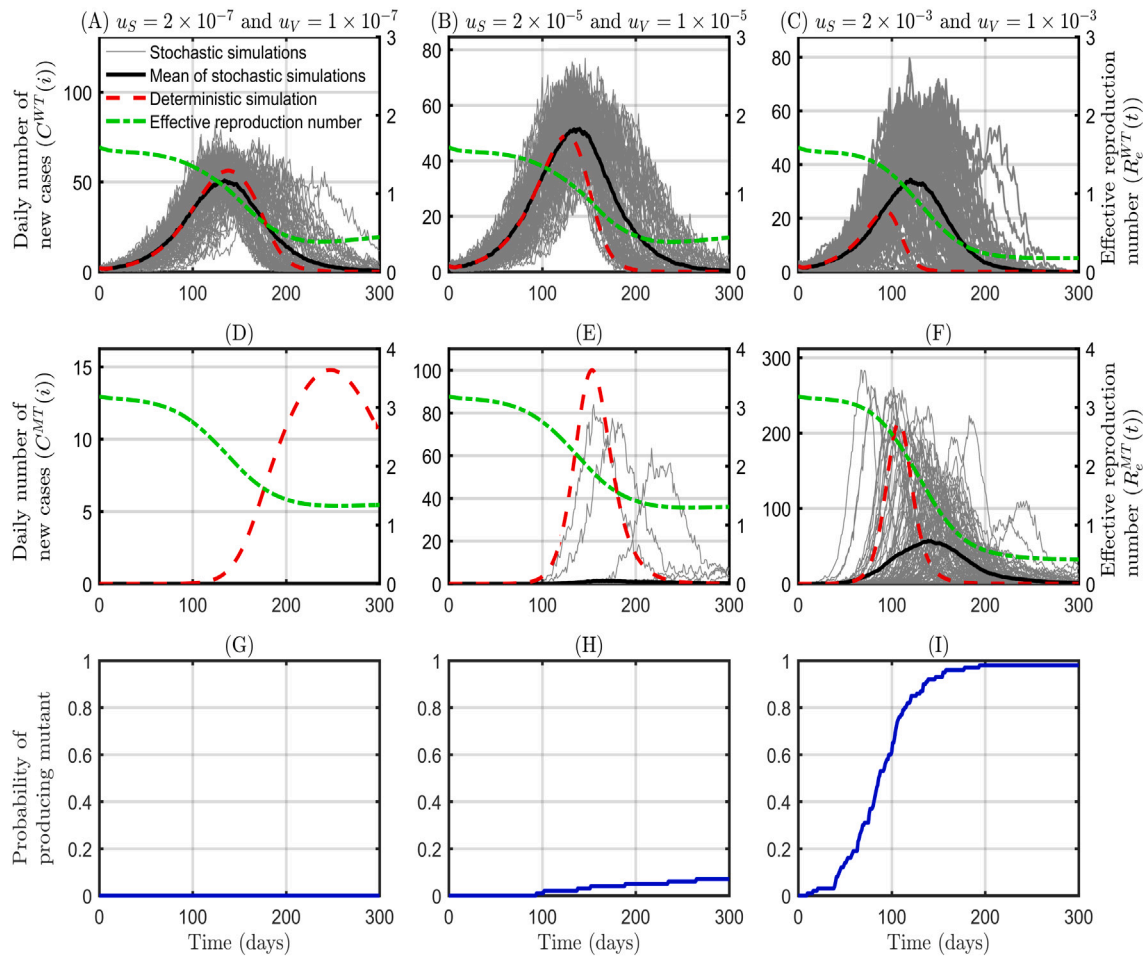
Fig. 1. The effect of mutation probability (u_S and u_V) on the probability of emergence of MT. The results of deterministic and 100 stochastic simulations of time series of WT (MT) when mutation probability is $u_S = 2 \times 10^{-7}$ and $u_V = 1 \times 10^{-7}$; $u_S = 2 \times 10^{-5}$ and $u_V = 1 \times 10^{-5}$; and $u_S = 2 \times 10^{-3}$ and $u_V = 1 \times 10^{-3}$ are shown in Subfigures A, B, and C (D, E, and F), respectively. Subfigures G, H, and I show the probability of producing a mutant strain over time, for the same values of u_S and u_V in the order specified above. Values of other parameters are $r_v = 0.6$, $r_{A_{WT}} = 0.05$, and $r_{I_{WT}} = 0.06$.

simulation. Our initial conditions above imply a total population $N(0)$ equal to 10 000. Our goal is to study the two stages of propagation of MT, including the emergence and spread of new variants. The effects of seven parameters on the transmission of resistant strains are explored: the mutation probability (u_S and u_V), perceived costs of vaccinators (r_v), and perceived risks of infection ($r_{A_{WT}}$, $r_{A_{MT}}$, $r_{I_{WT}}$, and $r_{I_{MT}}$).

3.1. Emergence of mutant strains

To assess the emergence of mutant strains of SARS-CoV-2, we define the probability of producing MT as the ratio of the number of stochastic simulations with more than one new case of MT to the total number of stochastic simulations that we performed. To do this, we defined a matrix A with dimensions $M \times T$, where M is the total number of stochastic simulations and T is the total number of days in each simulation. If the number of new cases of MT produced by a given stochastic simulation i exceeds one for the first time on day j, we define $A_{i,h} = 1$ for $h \geq j$ and $A_{i,h} = 0$ for $h < j$. Let P_j denote the probability that a mutant strain has been produced on or before day j. Obviously, we have

$$P_j = \frac{\sum_{i=1}^{M} A_{i,j}}{M}.$$

Each run of the model was done for a total time of 300 days, with vaccination starting on the first day. Since people have no perceived

risks to MT before it appears, we set $r_{A_{MT}} = r_{I_{MT}} = 0$. Then, we simulated the effects of mutation probability (u_S and u_V), perceived costs of vaccinators (r_v), and perceived risks of WT infection ($r_{A_{WT}}$ and $r_{I_{WT}}$) on the probability of producing MT (see Figs. 1, 2, and 3). At the same time, we also drew time series diagrams of proportion of vaccination, vaccine uptake, vaccinated cases, unvaccinated cases, susceptibles, and payoff function (see Figures C.1-C.6 of Appendix C). When the mutation probability (u_S and u_V) is very small, the numbers of simulated new cases in the stochastic version of the model are quite different compared to those in the deterministic version. This was particularly evident for MT; the differences between the time series of simulated new cases infected with WT for the stochastic and deterministic models were smaller (see Fig. 1). Our results show that stochastic simulation can better characterize whether or not MT emerges, as a new variant arising is guaranteed in the deterministic model.

Fig. 1 shows the results of deterministic and 100 stochastic simulations of WT and MT when the mutation probabilities in unvaccinated and vaccinated individuals are $u_S = 2 \times 10^{-7}$ and $u_V = 1 \times 10^{-7}$; $u_S = 2 \times 10^{-5}$ and $u_V = 1 \times 10^{-5}$; and $u_S = 2 \times 10^{-3}$ and $u_V = 1 \times 10^{-3}$, respectively. We find that the probability of producing MT in 100 stochastic simulations is only 0 when $u_S = 2 \times 10^{-7}$ and $u_V = 1 \times 10^{-7}$. In contrast, deterministic simulations with these values of u_S and u_V indicated that MT will emerge. The probability of producing MT in 100 stochastic simulations is instead 7% when $u_S = 2 \times 10^{-5}$ and $u_V = 1 \times 10^{-5}$; and 98% when $u_S = 2 \times 10^{-3}$ and $u_V = 1 \times 10^{-3}$. We also ran
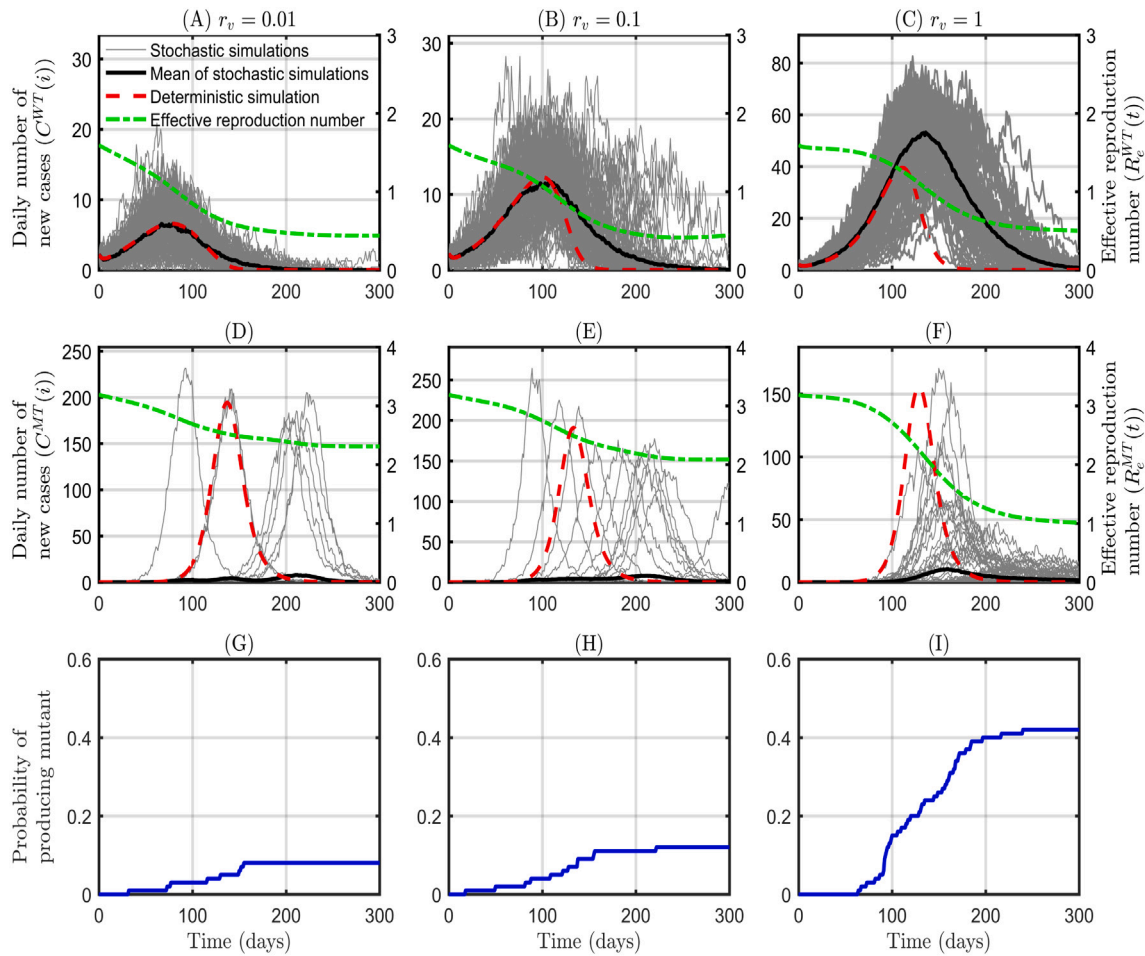
Fig. 2. The effect of perceived costs of vaccinators (r_v) on the probability of emergence of MT. The results of deterministic and 100 stochastic simulations of time series of WT (MT) when perceived costs of vaccinators are $r_v = 0.01$, $r_v = 0.1$, and $r_v = 1$ are shown in Subfigures A, B, and C (D, E, and F), respectively. Subfigures G, H, and I show the probability of producing a mutant strain over time, for the same values of r_v in the order specified above. Values of other parameters are $u_S = 2 \times 10^{-4}$, $u_V = 1 \times 10^{-4}$, $r_{A_{WT}} = 0.05$, and $r_{I_{WT}} = 0.06$.

simulations where we set the mutation probability to $u_S = 2 \times 10^{-4}$ and $u_V = 1 \times 10^{-4}$ and varied the perceived cost for vaccinators r_v. If this cost increases from 0.01 to 0.1, the probability of producing MT increases from 8% to 12%. A further order of magnitude increase, i.e. an increase from 0.01 to 1, will further increase the probability for MT to appear by about two fifths, as shown in Fig. 2. Hence, when $r_v = 1$, the chance that MT emerges is five times higher than when $r_v = 0.01$. This transforms the emergence of MT from a fairly uncommon event to a much more likely one. We also simulated cases in which we altered the perceived risks that arise from being infected. Specifically, we ran the deterministic and stochastic version of the model for $r_{A_{WT}} = 0.05$ and $r_{I_{WT}} = 0.1$; $r_{A_{WT}} = 0.1$ and $r_{I_{WT}} = 0.2$; and $r_{A_{WT}} = 0.4$ and $r_{I_{WT}} = 0.8$. In these three scenarios, the probabilities of producing MT in 100 stochastic simulations were 41%, 25%, and 9%, respectively, as shown in Fig. 3. Our analysis shows that mutation probability (u_S and u_V), perceived cost for vaccinators (r_v), and perceived risks of WT infection ($r_{A_{WT}}$ and $r_{I_{WT}}$) all have great impacts on the probability of producing MT. Changes in social norms can realize these impacts: the emergence of new variants can be effectively prevented by decreasing the perceived cost associated with vaccination (r_v) and increasing the perceived risks of WT infection ($r_{A_{WT}}$ and $r_{I_{WT}}$).

Next, we simulated the effect of the perceived cost of being vaccinated (r_v) and perceived risks of WT infection ($r_{A_{WT}}$ and $r_{I_{WT}}$) on the probability of producing MT under non-pharmaceutical interventions (i.e. by decreasing the transmission rate to decrease R_0). We assumed that these interventions were implemented in the first and second

months of the COVID-19 outbreak: we decreased the transmission rate by 80% in the first month and 60% in the second. (We took $u_S = 2 \times 10^{-4}$ and $u_V = 1 \times 10^{-4}$, and all other parameters as above.) When non-pharmaceutical interventions are implemented, if the perceived cost for vaccinators increases from 0.01 to 0.1 to 1, the probability of producing MT increases from 1% to 4% to 9%, as shown in Figure C.7 of Appendix C. This represented decreases in the probability of producing MT by 87.5%, 66.7%, and 78.6%, respectively, compared to the scenario without non-pharmaceutical interventions. As previously, we performed simulations when perceived risks of WT infection were $r_{A_{WT}} = 0.05$ and $r_{I_{WT}} = 0.1$; $r_{A_{WT}} = 0.1$ and $r_{I_{WT}} = 0.2$; and $r_{A_{WT}} = 0.4$ and $r_{I_{WT}} = 0.8$. There, the probability of producing MT (across 100 stochastic simulations) was 11%, 3%, and 2%, respectively, as shown in Figure C.10 of Appendix C. Again, these represent consistent improvements over the scenario without non-pharmaceutical interventions, with the greatest decline in MT emergence probability coming at intermediate perceived risk from WT.

We also evaluated the probability of MT emerging under various social norms and perceptions when the mutation rate was lower and non-pharmaceutical interventions were in place, which was accomplished by taking $u_S = 1 \times 10^{-4}$, $u_V = 5 \times 10^{-5}$ and all other parameters at their baseline values described above. For instance, we varied r_v, the perceived risk of being vaccinated. Under the reduced mutation rate, when the perceived cost for vaccinators is $r_v = 0.1$, MT did not appear in 100 stochastic simulations, as shown in Figure C.13 of Appendix C. This is because the non-pharmaceutical interventions made WT's effective
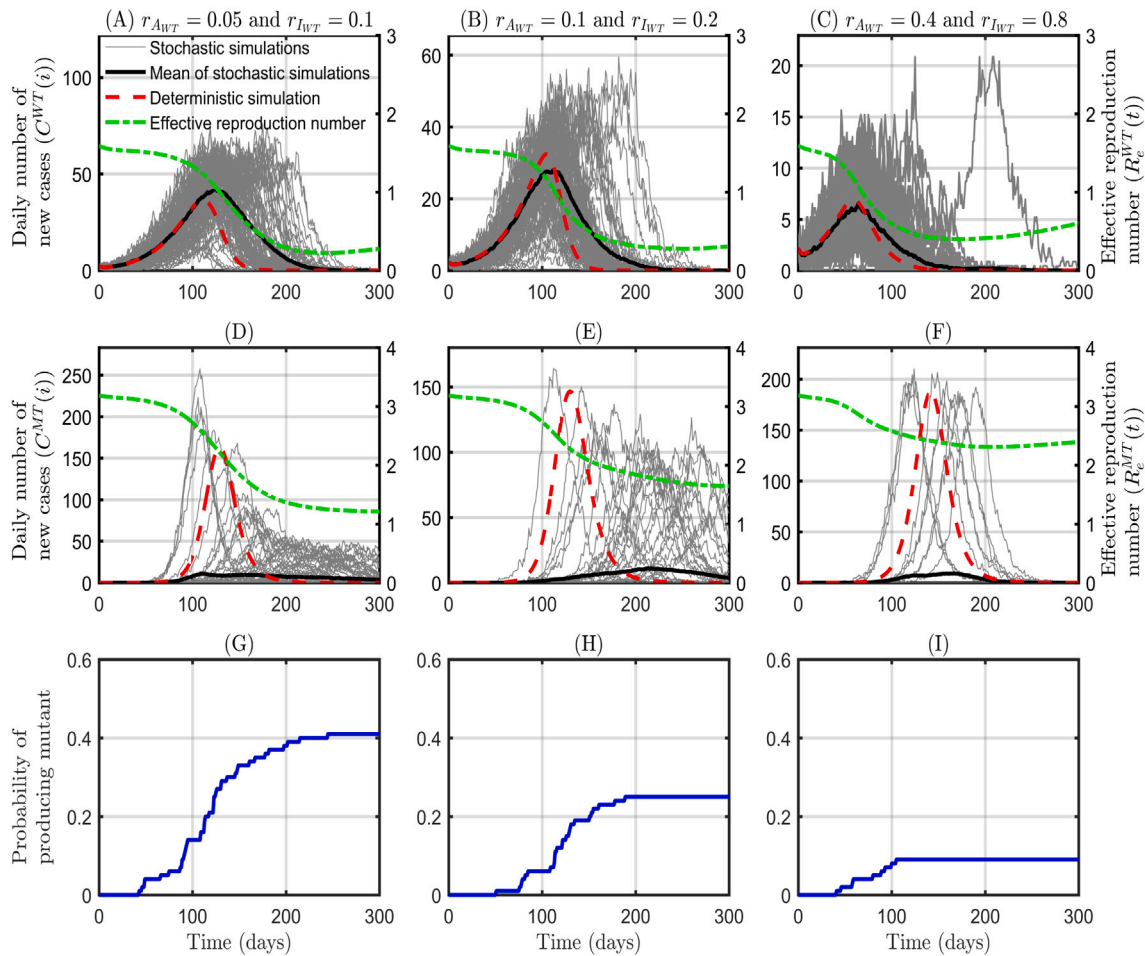
Fig. 3. The effect of perceived risks of WT infection ($r_{A_{WT}}$ and $r_{I_{WT}}$) on the probability of emergence of MT. The results of deterministic and 100 stochastic simulations of time series of WT (MT) when perceived risks of infection are $r_{A_{WT}} = 0.05$ and $r_{I_{WT}} = 0.1$; $r_{A_{WT}} = 0.1$ and $r_{I_{WT}} = 0.2$; and $r_{A_{WT}} = 0.4$ and $r_{I_{WT}} = 0.8$ are shown in Subfigures A, B, and C (D, E, and F), respectively. Subfigures G, H, and I show the probability of producing a mutant strain over time, for the same sets of values of $r_{A_{WT}}$ and $r_{I_{WT}}$, in the order specified above. Values of other parameters are $u_S = 2 \times 10^{-4}$, $u_V = 1 \times 10^{-4}$, and $r_v = 0.6$.

reproduction number $R_e^{WT}(t) < 1$ within a relatively short timeframe, which rapidly decreased the prevalence of WT and hence prevented the emergence of MT. In this low-mutation scenario, we also varied the perceived risks of WT infection. When $r_{A_{WT}}$ and $r_{I_{WT}}$ were 0.05 and 0.1; 0.1 and 0.2; and 0.4 and 0.8, the probability of producing MT was 4%, 3%, and 0%, respectively, as shown in Figure C.16 of Appendix C. MT therefore did not appear when perceived infection risk was high and non-pharmaceutical interventions were in place, as was the case when the perceived risk from being vaccinated was low. This shows that non-pharmaceutical interventions, in conjunction with vaccination, can be highly effective at preventing the emergence of potentially dangerous new virus variants.

3.2. Impact of perceived cost for vaccinators

Once MT had established itself, we used deterministic simulations to estimate disease prevalence trends after MT's emergence. We assessed the impact of the perceived cost of being vaccinated r_v on the burden of COVID-19 (measured in terms of the daily number of new cases, i.e., the daily incidence) by simulating Model (4) for different values of this cost. See Figure C.19 of Appendix C for the values which were used. The simulation results show that changes in the perceived cost for vaccinators have great impacts on COVID-19 incidence, as shown in Figure C.19. In particular, when mutation probability (u_S and u_V) is small, increasing r_v from 0 to 1 results in a drastic 95% decrease in disease incidence at MT's peak, a peak time of MT infection that

occurs more than 300 days later, and a very substantial decrease (close to 95%) in the total number of MT infections during the simulation. The peak size, peak time, and total number of cases of WT follow exactly opposite trends as those of MT infection, which is due to the fact that MT is more infective and rapidly replaces WT. In fact, Figs. 2, C.7, and C.19 together indicate that the total effect of increasing r_v (for small to intermediate values of u_S and u_V) is to make MT more likely to emerge, but also increase the harmful effects of WT once MT has already emerged. This effect corresponds to prolonging the WT wave while creating the MT wave. On the other hand, when the mutation probability (u_S and u_V) is large, the perceived cost for vaccinators impacts the characteristics of the MT outbreak on a much lesser scale. For example, when the mutation probability parameters (u_S and u_V) are taken to be 10^{-3} and 5×10^{-4}, respectively, increasing r_v from 0 to 1 will result in a 0.3% decrease in disease incidence when MT transmission peaks, a eight day delay in the peak time of MT, and a 12% decrease in the final size of MT. Our results show that the perceived risk associated with vaccination can have a large impact on how the WT and MT outbreaks unfold, albeit when the mutation probability (u_S and u_V) is sufficiently small.

3.3. Impact of perceived risks of WT infection

Near the beginning of an outbreak, the perceived risk associated with being infected by WT always influences how the outbreak develops. To investigate this within the context of a pandemic with emergent
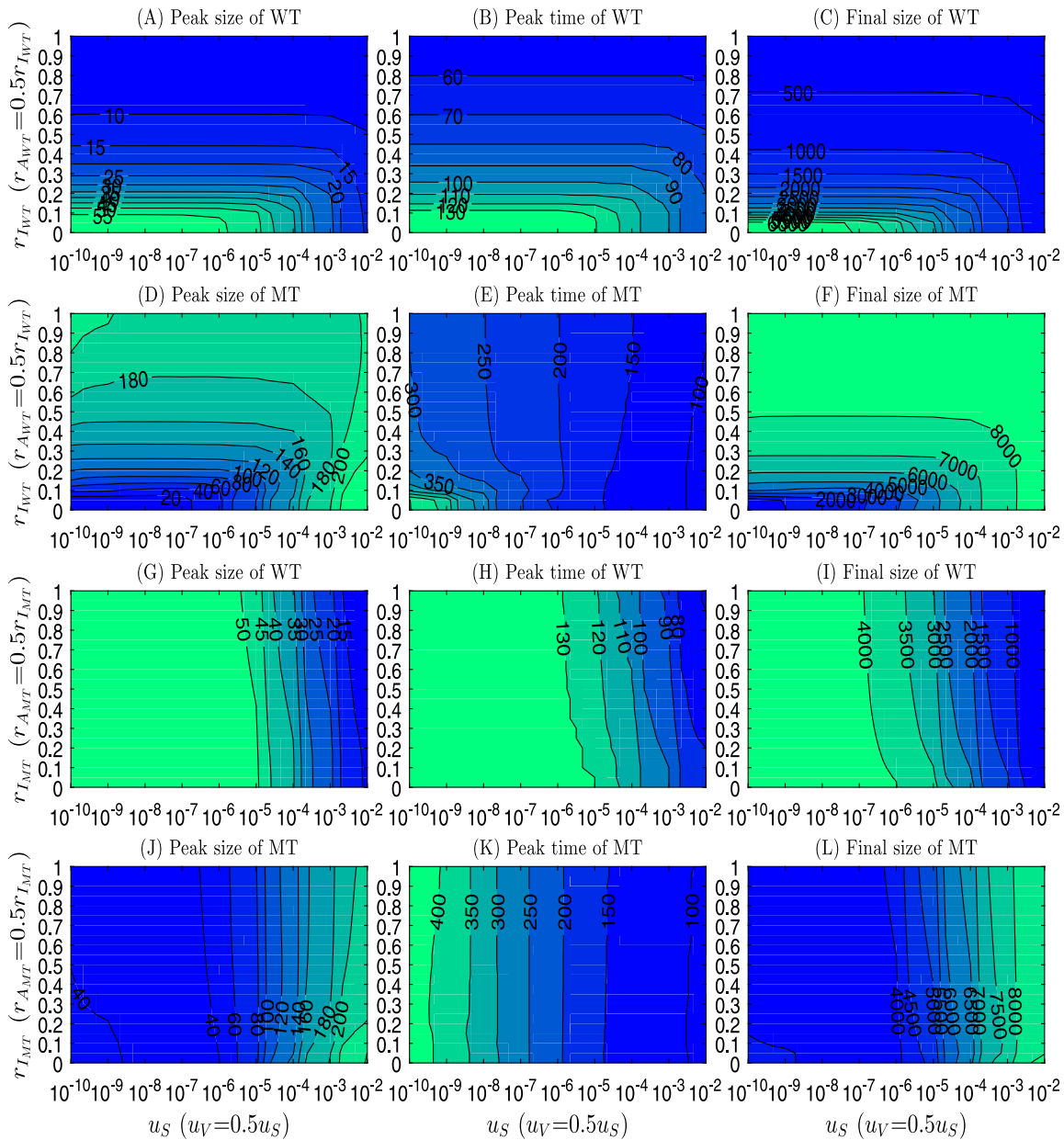
Fig. 4. Impact of perceived risks of WT (MT) infection and mutation probability on peak size, peak time, and final outbreak size for $r_{A_{MT}} = 0.05$ ($r_{A_{WT}} = 0.05$), $r_{I_{MT}} = 0.1$ ($r_{I_{WT}} = 0.1$), and $r_v = 0.6$. Subfigures A, B, and C (D, E, and F) show the peak number of daily infections, day when peak occurs, and total number of infections for WT (MT) with fixed parameters $r_{A_{MT}}$, $r_{I_{MT}}$, and r_v. Subfigures G, H, and I (J, K, and L) show the peak number of daily infections, day when peak occurs, and total number of infections for WT (MT) with fixed parameters $r_{A_{WT}}$, $r_{I_{WT}}$, and r_v.

viral strains, we simulated the model (4) for different values of the perceived risks of WT infection, i.e. $r_{A_{WT}}$ and $r_{I_{WT}}$ (see the top two rows of Fig. 4 for the values used). As with r_v, changes in the perceived risks of WT infection were found to have substantial impact on COVID-19 incidence, especially if the mutation probability (u_S and u_V) is small, as shown in the top two rows of Fig. 4. To illustrate this, when the two mutation probability parameters (u_S and u_V) are taken to be 10^{-8} and 5×10^{-9}, respectively, increasing the perceived risks of WT infection from 0 to 1 brought about a 32-fold increase in peak size of MT, a 132-day earlier peak time for MT, and a 6-fold increase in total number of people infected by MT at the end of our simulation. At the same time, this change in the perceived risks of WT infection also led to a 11-fold decrease in peak size, a 87-day earlier peak time, and a 19-fold decrease

in the final outbreak size of WT. When the mutation probability (u_S and u_V) is large, the impact of variation in $r_{A_{WT}}$ and $r_{I_{WT}}$ on the outbreak characteristics of WT is reduced but still substantial, and the impact on characteristics of MT becomes minimal. In particular, if the perceived risks of WT infection are increased from 0 to 1 and the mutation probability constants (u_S and u_V) are maintained at 10^{-3} and 5×10^{-4}, respectively, WT has an 80% lower infectivity peak which occurs 48 days earlier, and the final number of people infected by WT is 80% lower. For MT, this resulted in a 3% lower infectivity peak which occurs 12 days later, and 14% fewer total cases at the end of the simulation. This shows that if the perceived risk of WT infection is high, COVID-19 transmission can be slowed down and outbreaks can be controlled more effectively early on (while they are more manageable). Similarly, in this

scenario, increases in infections by MT can be traded off for decreases in infections by WT, in this way postponing the pandemic's effects while keeping total infections (WT plus MT) at a comparable level.

3.4. Impact of perceived risks of MT infection

Simulations of the model (4) were also carried out to investigate the impact of the perceived risks of MT infection ($r_{A_{MT}}$ and $r_{I_{MT}}$) on the peak size, peak time, and final number of infections with the different SARS-CoV-2 strains in our model (see the bottom two rows of Fig. 4). We found that regardless of the value chosen for mutation probability (u_S and u_V), the impact of changes in the perceived risks of MT infection on characteristics of the WT and MT outbreaks were minor compared to the impact of varying $r_{A_{WT}}$ and $r_{I_{WT}}$, as shown in the bottom two rows of Fig. 4. This can be illustrated with the examples of $u_S = 10^{-3}$ ($u_V = 5 \times 10^{-4}$) and $u_S = 10^{-8}$ ($u_V = 5 \times 10^{-9}$). In the former case, increasing the perceived risks of MT infection from 0 to 1 caused a 15% decrease in peak height, no change in peak time, and a 8% decrease in final outbreak size for MT, and a $1.2 \times 10^{-2}\%$ decrease in peak height, no change in peak time, and a $9.2 \times 10^{-2}\%$ decrease in the final outbreak size for WT. In the latter case, the corresponding numbers were a 14% decrease in peak size, a delay of two days for peak time, and a 0.4% increase in total infections for MT, as well as a 17% decrease in peak size, a peak of infection 12 days earlier, and a decrease in the final outbreak size by 28% for WT. This, in conjunction with our previous analysis, shows that public perceptions of WT have more impact than those of MT on shaping the courses of both the WT and MT outbreaks.

4. Discussion

To understand the emergence and spread of SARS-CoV-2 variants, we developed a dynamic game model featuring two such variants (WT and MT), which assumes that vaccination decisions are made according to disease prevalence (i.e. the number of new cases) and the perceived risks of vaccines and disease. We applied semi-stochastic simulations to estimate the probability of the emergence of MT, since such an event, and in particular MT's non-extinction due to random drift, is stochastic by nature. We simulated the effect of mutation probability, perceived costs of vaccinators, and perceived risks of infection on the probability of producing MT. After this, to assess the impact of this perceived costs on the burden of COVID-19 (measured in terms of the daily number of new cases), we also ran the model for different values of the perceived cost of being vaccinated (r_v) and the perceived risks of WT infection ($r_{A_{WT}}$ and $r_{I_{WT}}$). Using this method, we find that decreasing the perceived risk from vaccination and increasing that from infection will prevent the emergence of new variants. Our results also show that lower perceived vaccination risk can minimize the number of WT cases that occur after MT has appeared, highlighting how promoting vaccine uptake can reduce pandemic-related harm in multiple orthogonal ways.

We found that after the emergence of MT, the perceived risks associated with being infected by WT (i.e. $r_{A_{WT}}$ and $r_{I_{WT}}$) played a large role in determining the characteristics of both the WT and MT outbreaks going forward. However, the corresponding risks associated with MT (i.e. $r_{A_{MT}}$ and $r_{I_{MT}}$) had much lesser, and in some cases negligible, impact on the shape of the epidemic curves of WT and MT. This indicates that when a new variant of SARS-CoV-2 begins to appear, public perception of the variant that is dominant at the time is highly important in shaping the epidemiological trajectory of the new one. These results suggest that although public concern over Omicron surged mere days after that variant was first observed (Su et al., 2022), this upsurge in concern was likely less effective in preventing Omicron cases than closer adherence to individual-level precautions against Delta would have been.

One possible explanation for this is that the relatively greater number of WT cases during the emergence of MT is more responsible for

driving the payoff function ΔF. This is evident because ΔF tends to reach its maximum at the same time as the peak of the WT outbreak wave, and can be seen in Figs. 1 and C.2, or 2 and C.4, or 3 and C.6. This finding also may be because the same mutations that generate a new variant can happen on multiple independent occasions in our model, allowing more MT cases to be generated when MT transmission is high. This phenomenon has been seen during the COVID-19 pandemic, where a few notable mutations of interest (for example D614G) have been shared among many different lineages (Fan et al., 2021), indicating that the same mutation can arise many times under different contexts.

The notion that individual-level risk assessment can substantially alter the course of a pandemic has previously been observed on multiple occasions. The term "pandemic fatigue" entered the lexicon in 2020 (Reicher and Drury, 2021), and studies from later in the pandemic found that many people had reduced their behavioural precautions against SARS-CoV-2 infection (Haktanir et al., 2021), particularly with regards to physical distancing (Petherick et al., 2021). Similar reductions in social distancing behaviour over time were also observed in Hong Kong during the 2009 H1N1 pandemic, which were directly attributed to people becoming less concerned about a possible infection (Cowling et al., 2010). These were contemporary with a steady increase (but perceived decrease) in case numbers there during the summer of 2009. This highlights the possibility of being over-vigilant at the beginning of an outbreak wave but experiencing burnout near the end of one.

Our results show that higher perceived risk associated with receiving vaccines (i.e. higher values for r_v) is associated with a higher probability of new variants emerging (Figs. 2 and C.7 of Appendix C). High values of r_v were also associated with the WT outbreak being more severe in relation to the MT outbreak after MT has become established (Figure C.19 of Appendix C). However, if r_v is low, it becomes more likely that the number of MT infections both at the peak of its outbreak and overall is zero, as shown in our stochastic simulations. After accounting for this, higher values of r_v correspond to greater expected caseloads both for WT and for MT. During the first half of 2021, substantial populations in many countries expressed unwillingness to receive a vaccine (Ritchie et al., 2020; Cooper et al., 2021; Köhler et al., 2021). This was followed by a global increase in COVID-19 cases later in 2021, caused by the Delta variant. As the vaccines in use at the time offered at least moderate protection against Delta (Bian et al., 2021), in countries such as the United States with high vaccine supply but lower uptake, this elevated number of caseloads can be attributed at least in part to prior vaccine hesitancy. This emphasizes the importance of reducing misinformation that could lead to lower vaccine uptake, as suggested by our model.

We also note that the changes in epidemiological characteristics of MT and WT in our model brought about by variation in $r_{A_{WT}}$ and $r_{I_{WT}}$ plateaued at much smaller values compared to the changes due to variation in r_v. Therefore, we believe that treating COVID-19 infection as a moderate risk is necessary, but efforts beyond that level should mainly be devoted to encouraging vaccination. This is especially pertinent in China, which recently transitioned away from a zero-Covid strategy and subsequently experienced a large wave of infections. Because booster dose administration in China is currently at much lower levels than it was earlier in the pandemic (Ritchie et al., 2020), we believe that encouraging vaccination in China would significantly help prevent new variants from emerging in the future.

We also simulated the effect of the perceived cost borne by people choosing to get vaccinated (r_v) and the perceived risks associated with infection by each variant ($r_{A_{WT}}$ and $r_{I_{WT}}$) on the probability of producing MT under non-pharmaceutical interventions. It has previously been found that vaccination and non-pharmaceutical interventions have large interaction effects on lowering the infectivity of different SARS-CoV-2 variants (Ge et al., 2022a,b; Layton and Sadria, 2022); we further extend this to show that the combination of vaccination and non-pharmaceutical interventions is more effective at

decreasing the probability of producing new variants. Because of the synergy that exists between these two strategies, governments can both reduce infection by existing SARS-CoV-2 variants and delay or even prevent the emergence of vaccine-resistant mutant variants by reducing vaccine hesitancy and using targeted non-pharmaceutical measures. Efficacy of vaccination can wax and wane depending on how similar the variants that available vaccines were first developed for are to the variants that are in circulation at a given time (see e.g. Zhang et al., 2021), while non-pharmaceutical interventions provide a more static form of controlling infectivity. These two control methods also act over different timescales. Vaccine development and clinical trials take a great deal of time, whereas non-pharmaceutical interventions over comparatively shorter intervals can be effective (see Figures C.7 and C.10 of Appendix C). Thus, the two methods can complement each other in a government's toolbox when planning long-term COVID-19 responses.

Our study still has several limitations. First, we did not take into account the seasonality of infection patterns, i.e. we only simulated one large outbreak of COVID-19. Second, we assumed that the whole population can be vaccinated, and vaccines can neither reduce the transmissibility nor shorten the infection period. Third, we did not consider age heterogeneity and the evolution of the virus within the host. Fourth, we assumed that a single strain of SARS-CoV-2 would be dominant at the time MT emerged, and that this dominant strain would be less infective and more lethal than MT. Additionally, we did not differentiate between multiple doses of vaccination. Also, we did not parameterize our model with the actual number of cases in any one particular country, instead opting to use parameter values broadly characteristic of outbreaks seen around the world thus far. Future work will address these issues by incorporating time-dependent trends such as temporal fluctuation in patterns of contact, as well as simulating conditions in specific jurisdictions.

In conclusion, we have developed a model that couples the framework of compartmental disease transmission with game theoretical dynamics on whether or not to vaccinate. Our dynamic game model is used to describe the proportion of people willing to be vaccinated, as it captures the risk evaluation inherent in this decision, while semi-stochastic simulations are used to explore the emergence of new variants because of the inherent randomness of mutations. The probability of emergence of a vaccine-resistant mutant strain of SARS-CoV-2 (MT) mainly depends on the number of confirmed cases due to the wild-type virus (WT), but this probability can be substantially altered by factors both upstream and downstream from WT caseloads. Chief among these are the perceptions of risk due to WT infection and due to vaccination. Because of interaction effects between non-pharmaceutical interventions and public support for vaccination, rapid vaccination under non-pharmaceutical interventions can delay or even prevent the emergence of a new variant. Our results suggest that the correction of vaccine-related negative information and non-pharmaceutical interventions (such as reducing social contact) will have orthogonal, compounding effects on avoiding the establishment of new variants. Hence, a successful strategy for variant prevention would combine both of these.

CRediT authorship contribution statement

Shuanglin Jing: Conceptualization, Methodology, Software, Formal analysis, Investigation, Writing – original draft, Visualization. **Russell Milne:** Conceptualization, Software, Writing – original draft, Writing – review & editing, Visualization, Supervision. **Hao Wang:** Conceptualization, Methodology, Writing – review & editing, Supervision, Project administration, Funding acquisition. **Ling Xue:** Supervision, Project administration, Funding acquisition.

Declaration of competing interest

The authors declare that they have no known competing financial interests or personal relationships that could have appeared to influence the work reported in this paper.

Acknowledgements

Appendix A. Supplementary data

Supplementary material related to this article can be found online at https://doi.org/10.1016/j.jtbi.2023.111522.

References

Akinbami, L.J., Kruszon-Moran, D., Wang, C.-Y., Storandt, R.J., Clark, J., Riddles, M.K., Mohadjer, L.K., 2022. SARS-CoV-2 serology and self-reported infection among adults—National health and nutrition examination survey, United States, august 2021–may 2022. Morb. Mortal. Wkly. Rep. 71 (48), 1522–1525.

Al Kaabi, N., Zhang, Y., Xia, S., Yang, Y., Al Qahtani, M.M., Abdulrazzaq, N., Al Nusair, M., Hassany, M., Jawad, J.S., Abdalla, J., et al., 2021. Effect of 2 inactivated SARS-CoV-2 vaccines on symptomatic COVID-19 infection in adults: a randomized clinical trial. JAMA 326 (1), 35–45.

Barouch, D.H., Stephenson, K.E., Sadoff, J., Yu, J., Chang, A., Gebre, M., McMahan, K., Liu, J., Chandrashekar, A., Patel, S., et al., 2021. Durable humoral and cellular immune responses 8 months after Ad26. COV2. s vaccination. N. Engl. J. Med. 385 (10), 951–953.

Bauch, C.T., 2005. Imitation dynamics predict vaccinating behaviour. Proc. R. Soc. B 272 (1573), 1669–1675.

Bauch, C.T., Earn, D.J., 2004. Vaccination and the theory of games. Proc. Natl. Acad. Sci. 101 (36), 13391–13394.

Bian, L., Gao, Q., Gao, F., Wang, Q., He, Q., Wu, X., Mao, Q., Xu, M., Liang, Z., 2021. Impact of the Delta variant on vaccine efficacy and response strategies. Expert Rev. Vaccines 20 (10), 1201–1209.

Bordon, Y., 2022. Social distancing plus rapid vaccination prevents emergence of SARS-CoV-2 variants. Nat. Rev. Immunol. 22 (4), 208.

Brisson, M., Edmunds, W.J., 2003. Economic evaluation of vaccination programs: the impact of herd-immunity. Med. Decis. Mak. 23 (1), 76–82.

Cai, Y., Zhang, J., Xiao, T., Lavine, C.L., Rawson, S., Peng, H., Zhu, H., Anand, K., Tong, P., Gautam, A., et al., 2021. Structural basis for enhanced infectivity and immune evasion of SARS-CoV-2 variants. Science 373 (6555), 642–648.

Cao, Y., Wang, J., Jian, F., Xiao, T., Song, W., Yisimayi, A., Huang, W., Li, Q., Wang, P., An, R., et al., 2022. Omicron escapes the majority of existing SARS-CoV-2 neutralizing antibodies. Nature 602 (7898), 657–663.

Cele, S., Jackson, L., Khoury, D.S., Khan, K., Moyo-Gwete, T., Tegally, H., San, J.E., Cromer, D., Scheepers, C., Amoako, D.G., et al., 2022. Omicron extensively but incompletely escapes pfizer BNT162b2 neutralization. Nature 602 (7898), 654–656.

Centers for Disease Control and Prevention, 2022. COVID data tracker. Available from: https://covid.cdc.gov/covid-data-tracker/#variant-proportions, Accessed 21 December 2022.

Cooper, S., van Rooyen, H., Wiysonge, C.S., 2021. COVID-19 vaccine hesitancy in South Africa: how can we maximize uptake of COVID-19 vaccines? Expert Rev. Vaccines 20 (8), 921–933.

Cowling, B.J., Ng, D.M.W., Ip, D.K.M., Liao, Q., Lam, W.W.T., Wu, J.T., Lau, J.T.F., Griffiths, S.M., Fielding, R., 2010. Community psychological and behavioral responses through the first wave of the 2009 influenza A(H1N1) pandemic in Hong Kong. J. Infect. Dis. 202 (6), 867–876.

Deka, A., Bhattacharyya, S., 2022. The effect of human vaccination behaviour on strain competition in an infectious disease: An imitation dynamic approach. Theor. Popul. Biol. 143, 62–76.

Deka, A., Pantha, B., Bhattacharyya, S., 2020. Optimal management of public perceptions during a flu outbreak: A game-theoretic perspective. Bull. Math. Biol. 82 (11), 1–23.

Del Rio, C., Malani, P.N., Omer, S.B., 2021. Confronting the delta variant of SARS-CoV-2, summer 2021. JAMA 326 (11), 1001–1002.

Dong, Y., Mo, X., Hu, Y., Qi, X., Jiang, F., Jiang, Z., Tong, S., 2020. Epidemiology of COVID-19 among children in China. Pediatrics 145 (6), e20200702.

Elliott, P., Eales, O., Steyn, N., Tang, D., Bodinier, B., Wang, H., Elliott, J., Whitaker, M., Atchison, C., Diggle, P.J., Page, A.J., Trotter, A.J., Ashby, D., Barclay, W., Taylor, G., Ward, H., Darzi, A., Cooke, G.S., Donnelly, C.A., Chadeau-Hyam, M., 2022. Twin peaks: The omicron SARS-CoV-2 BA.1 and BA.2 epidemics in England. Science 376 (6600).

Fan, L., Hu, X., Chen, Y., Peng, X., Fu, Y., Zheng, Y., Yu, J., He, J., 2021. Biological significance of the genomic variation and structural dynamics of SARS-CoV-2 B.1.617. Front. Microbiol. 12, 750725.

Faust, J.S., Del Rio, C., 2020. Assessment of deaths from COVID-19 and from seasonal influenza. JAMA Internal Med. 180 (8), 1045–1046.

Gandon, S., Lion, S., 2022. Targeted vaccination and the speed of SARS-CoV-2 adaptation. Proc. Natl. Acad. Sci. 119 (3), e2110666119.

Ge, Y., Zhang, W.-B., Liu, H., Ruktanonchai, C.W., Hu, M., Wu, X., Song, Y., Ruktanonchai, N.W., Yan, W., Cleary, E., Feng, L., Li, Z., Yang, W., Liu, M., Tatem, A.J., Wang, J.-F., Lai, S., 2022a. Impacts of worldwide individual non-pharmaceutical interventions on COVID-19 transmission across waves and space. Int. J. Appl. Earth Obs. Geoinf. 106, 102649.

Ge, Y., Zhang, W.-B., Wu, X., Ruktanonchai, C.W., Liu, H., Wang, J., Song, Y., Liu, M., Yan, W., Yang, J., Cleary, E., Qader, S.H., Atuhaire, F., Ruktanonchai, N.W., Tatem, A.J., Lai, S., 2022b. Untangling the changing impact of non-pharmaceutical interventions and vaccination on European COVID-19 trajectories. Nature Commun. 13 (1), 1–9.

Gillespie, D.T., 1977. Exact stochastic simulation of coupled chemical reactions. J. Phys. Chem. 81 (25), 2340–2361.

Grenfell, B.T., Pybus, O.G., Gog, J.R., Wood, J.L., Daly, J.M., Mumford, J.A., Holmes, E.C., 2004. Unifying the epidemiological and evolutionary dynamics of pathogens. Science 303 (5656), 327–332.

Gutierrez, M.A., Gog, J.R., 2023. The importance of vaccinated individuals to population-level evolution of pathogens. J. Theoret. Biol. 567, 111493.

Haktanir, A., Can, N., Seki, T., Kurnaz, M.F., Dilmaç, B., 2021. Do we experience pandemic fatigue? current state, predictors, and prevention. Curr. Psychol. 1–12.

Hao, X., Cheng, S., Wu, D., Wu, T., Lin, X., Wang, C., 2020. Reconstruction of the full transmission dynamics of COVID-19 in wuhan. Nature 584 (7821), 420–424.

Köhler, T., English, R., Christian, C., 2021. Trends in COVID-19 public health intervention adherence and vaccine hesitancy in South Africa: 2020–2021. South Afr. Health Rev. 2021 (1), 274–285.

Kumar, N., AbdulRahman, A., AlAli, S., Otoom, S., Atkin, S.L., AlQahtani, M., 2021. Time till viral clearance of severe acute respiratory syndrome coronavirus 2 is similar for asymptomatic and non-critically symptomatic individuals. Front. Med. 8, 616927.

Layton, A.T., Sadria, M., 2022. Understanding the dynamics of SARS-CoV-2 variants of concern in Ontario, Canada: a modeling study. Sci. Rep. 12 (1), 2114.

Li, Q., Guan, X., Wu, P., Wang, X., Zhou, L., Tong, Y., Ren, R., Leung, K.S., Lau, E.H., Wong, J.Y., Xing, X., Xiang, N., Wu, Y., Li, C., Chen, Q., Li, D., Liu, T., Zhao, J., Liu, M., Tu, W., Chen, C., Jin, L., Yang, R., Wang, Q., Zhou, S., Wang, R., Liu, H., Luo, Y., Liu, Y., Shao, G., Li, H., Tao, Z., Yang, Y., Deng, Z., Liu, B., Ma, Z., Zhang, Y., Shi, G., Lam, T.T., Wu, J.T., Gao, G.F., Cowling, B.J., Yang, B., Leung, G.M., Feng, Z., 2020a. Early transmission dynamics in wuhan, china, of novel coronavirus–infected pneumonia. N. Engl. J. Med. 382 (13), 1199–1207.

Li, R., Pei, S., Chen, B., Song, Y., Zhang, T., Yang, W., Shaman, J., 2020b. Substantial undocumented infection facilitates the rapid dissemination of novel coronavirus (SARS-CoV-2). Science 368 (6490), 489–493.

Lo, N.C., Hotez, P.J., 2017. Public health and economic consequences of vaccine hesitancy for measles in the United States. JAMA Pediatr. 171 (9), 887.

Lobinska, G., Pauzner, A., Traulsen, A., Pilpel, Y., Nowak, M.A., 2022. Evolution of resistance to COVID-19 vaccination with dynamic social distancing. Nat. Hum. Behav. 6 (2), 193–206.

Maslo, C., Friedland, R., Toubkin, M., Laubscher, A., Akaloo, T., Kama, B., 2022. Characteristics and outcomes of hospitalized patients in South Africa during the COVID-19 Omicron wave compared with previous waves. JAMA 327 (6), 583–584.

McCallum, M., Walls, A.C., Sprouse, K.R., Bowen, J.E., Rosen, L.E., Dang, H.V., De Marco, A., Franko, N., Tilles, S.W., Logue, J., et al., 2021. Molecular basis of immune evasion by the delta and kappa SARS-CoV-2 variants. Science 374 (6575), 1621–1626.

McLeod, D.V., Gandon, S., 2022. Effects of epistasis and recombination between vaccine-escape and virulence alleles on the dynamics of pathogen adaptation. Nat. Ecol. Evol. 6 (6), 786–793.

Mizumoto, K., Kagaya, K., Zarebski, A., Chowell, G., 2020. Estimating the asymptomatic proportion of coronavirus disease 2019 (COVID-19) cases on board the diamond princess cruise ship, Yokohama, Japan, 2020. Eurosurveillance 25 (10), 2000180.

Murray, C.J., 2022. COVID-19 will continue but the end of the pandemic is near. Lancet 399 (10323), 417–419.

Pananos, A.D., Bury, T.M., Wang, C., Schonfeld, J., Mohanty, S.P., Nyhan, B., Salathé, M., Bauch, C.T., 2017. Critical dynamics in population vaccinating behavior. Proc. Natl. Acad. Sci. 114 (52), 13762–13767.

Pegu, A., O'Connell, S.E., Schmidt, S.D., O'Dell, S., Talana, C.A., Lai, L., Albert, J., Anderson, D., Bennett, H., Corbett, K.S., et al., 2021. Durability of mRNA-1273 vaccine–induced antibodies against SARS-CoV-2 variants. Science 373 (6561), 1372–1377.

Petherick, A., Goldszmidt, R., Andrade, E.B., Furst, R., Hale, T., Pott, A., Wood, A., 2021. A worldwide assessment of changes in adherence to COVID-19 protective behaviours and hypothesized pandemic fatigue. Nat. Hum. Behav. 5 (9), 1145–1160.

Pharaon, J., Bauch, C.T., 2018. The influence of social behaviour on competition between virulent pathogen strains. J. Theoret. Biol. 455, 47–53.

Planas, D., Saunders, N., Maes, P., Guivel-Benhassine, F., Planchais, C., Buchrieser, J., Bolland, W.-H., Porrot, F., Staropoli, I., Lemoine, F., et al., 2022. Considerable escape of SARS-CoV-2 omicron to antibody neutralization. Nature 602 (7898), 671–675.

Poland, G.A., Jacobson, R.M., 2001. Understanding those who do not understand: a brief review of the anti-vaccine movement. Vaccine 19 (17–19), 2440–2445.

Qiu, J., 2020. Covert coronavirus infections could be seeding new outbreaks. Nature http://dx.doi.org/10.1038/d41586-020-00822-x.

Reicher, S., Drury, J., 2021. Pandemic fatigue? How adherence to COVID-19 regulations has been misrepresented and why it matters. BMJ 372, n137.

Rella, S.A., Kulikova, Y.A., Dermitzakis, E.T., Kondrashov, F.A., 2021. Rates of SARS-CoV-2 transmission and vaccination impact the fate of vaccine-resistant strains. Sci. Rep. 11 (1), 1–10.

Ritchie, H., Mathieu, E., Rods-Guirao, L., Appel, C., Giattino, C., Ortiz-Ospina, E., Hasell, J., Macdonald, B., Beltekian, D., Roser, M., 2020. Coronavirus pandemic (COVID-19). Our World Data https://ourworldindata.org/coronavirus.

Su, Z., McDonnell, D., Ahmad, J., Cheshmehzangi, A., Xiang, Y.-T., 2022. Mind the "worry fatigue" amid Omicron scares. Brain Behav. Immun. 101, 60–61.

Tang, B., Zhou, W., Wang, X., Wu, H., Xiao, Y., 2022. Controlling multiple COVID-19 epidemic waves: an insight from a multi-scale model linking the behaviour change dynamics to the disease transmission dynamics. Bull. Math. Biol. 84 (10), 106.

Tegally, H., Moir, M., Everatt, J., Giovanetti, M., Scheepers, C., Wilkinson, E., Subramoney, K., Makatini, Z., Moyo, S., Amoako, D.G., et al., 2022. Emergence of SARS-CoV-2 omicron lineages BA. 4 and BA. 5 in South Africa. Nat. Med. 28 (9), 1785–1790.

Tegally, H., Wilkinson, E., Giovanetti, M., Iranzadeh, A., Fonseca, V., Giandhari, J., Doolabh, D., Pillay, S., San, E.J., Msomi, N., et al., 2021. Detection of a SARS-CoV-2 variant of concern in South Africa. Nature 592 (7854), 438–443.

Thomas, S.J., Moreira, Jr., E.D., Kitchin, N., Absalon, J., Gurtman, A., Lockhart, S., Perez, J.L., Pérez Marc, G., Polack, F.P., Zerbini, C., et al., 2021. Safety and efficacy of the BNT162b2 mRNA COVID-19 vaccine through 6 months. N. Engl. J. Med. 385 (19), 1761–1773.

Thompson, R.N., Hill, E.M., Gog, J.R., 2021. SARS-CoV-2 incidence and vaccine escape. Lancet Infect. Dis. 21 (7), 913–914.

Wang, X., Xiao, Y., Wang, J., Lu, X., 2012. A mathematical model of effects of environmental contamination and presence of volunteers on hospital infections in China. J. Theoret. Biol. 293, 161–173.

World Health Organization, 2022. WHO coronavirus (COVID-19) dashboard. Available from: https://covid19.who.int/, Accessed 21 December 2022.

Xiao, Y., Clancy, D., French, N.P., Bowers, R.G., 2006. A semi-stochastic model for Salmonella infection in a multi-group herd. Math. Biosci. 200 (2), 214–233.

Xue, L., Jing, S., Zhang, K., Milne, R., Wang, H., 2022. Infectivity versus fatality of SARS-CoV-2 mutations and influenza. Int. J. Infect. Dis. 121, 195–202.

Yang, S., Li, Y., Dai, L., Wang, J., He, P., Li, C., Fang, X., Wang, C., Zhao, X., Huang, E., et al., 2021. Safety and immunogenicity of a recombinant tandem-repeat dimeric RBD-based protein subunit vaccine (ZF2001) against COVID-19 in adults: two randomised, double-blind, placebo-controlled, phase 1 and 2 trials. Lancet Infect. Dis. 21 (8), 1107–1119.

Zhang, Y., Quigley, A., Wang, Q., MacIntyre, C.R., 2021. Non-pharmaceutical interventions during the roll out of COVID-19 vaccines. BMJ n2314.

Zhao, S., Wang, K., Chong, M.K., Musa, S.S., He, M., Han, L., He, D., Wang, M.H., 2022. The non-pharmaceutical interventions may affect the advantage in transmission of mutated variants during epidemics: A conceptual model for COVID-19. J. Theor. Biol. 542, 111105.